# **Determining a Length Scale of FRP Composite Microstructures**

MATHEW J. SCHEY, SCOTT E. STAPLETON, CRAIG P. PRZYBYLA, MICHAEL UCHIC and SIMON ZABLER

#### **ABSTRACT**

Carbon fiber reinforced plastics (CFRPs) have become the material of choice for many low weight, high strength applications. One problem associated with these materials is a scatter of mechanical properties. Efforts have been made to correlate these results with random fiber packing using 2-D representative volume elements (RVEs). While these efforts have shown that fiber distribution is important, scans have shown fiber position is a function of 3-D morphology. For example, fiber meandering and entanglement can only be seen when variation along the fiber direction is studied. While the optimal scale for 2-D RVEs is well researched, little has been done to find the effective length in which the 3-D behavior of real samples can be observed. As such, the construction and analysis of 3-D RVEs with a requisite length in the fiber direction is necessary.

The scope of this work is to study the fibers within a CFRP sample in order to recreate the microstructure. In this work, long micro-CT scans from an aerospace-grade are used to obtain the fiber positions. In addition, scans from an automotive grade specimen with a high fiber count manufactured using VARTM were analyzed due to the high potential for entanglement. Descriptive metrics were then generated to fiber behavior within both samples. The variance of these metrics was captured using the change in Pearson's Correlation Coefficient (R) with respect to position along the fiber length. One

<sup>&</sup>lt;sup>1</sup> Mathew J. Schey, Scott E Stapleton, University of Massachusetts Lowell, Lowell MA, USA Craig P. Przybyla, Michael Uchic, Air Force Research Laboratory, Dayton OH, USA Simon Zabler, Fraunhofer Institute for Integrated Circuits IIS, Würzburg, Germany

definition of the effective length is the distance after which R is less than 0.5 (i.e. the metric is no longer correlated to length). Using the long micro-CT scans, the effective length for each metric was determined. By establishing the optimal length for 3D RVEs, the true nature of CFRP microstructures can move closer to being understood.

#### **METHODS**

Two image stacks were made for two different composite microstructures. The first was made from aerospace-grade materials and high-pressure consolidation, while the other used more economical automotive-grade materials and processes. In this section, the materials and manufacturing methods will be discussed, along with details of the images. Additionally, the metrics for comparison will be outlined.

#### **Aerospace Scans**

The aerospace-grade composite materials were constructed from an IM7/5320-1 unidirectional prepreg. The specimen was a curved bracket geometry, with a 13 layer quasi-isotropic layup. The entire scan was taken at the Air Force Research Lab using their robotic serial sectioning system (LEROY). The system polishes the surface of the specimen, takes an image, then continues polishing. One of the main benefits of the system over micro CT is that large images can be taken with a high resolution, and high contact between fiber and matrix can be maintained. The resolution of the images was 0.336 µm/px, and images were taken with an average spacing of 1.07 µm between images. A total of 208 images were taken, and images were 4844 x 5939 px. Due to the physical constraints on LEROY the length of the imaged sample was only around 0.3 mm. As such the 90° layers (with fiber lengths of ~2 mm) were utilized after being rotated and scaled in ImageJ. Figure 1 shows the entire process of rotating and scaling the images. A significant downside to this way of imaging is also seen in Figure 1: the amount of material polished off after each scan varies. In the rotated images, this effectively skews the resolution according to the uneven spacing of the unrotated images. A MATLAB script was written to adjust the image resolution according to the approximate spacing provided by AFRL, but it is important to note that the results of this method are imperfect.

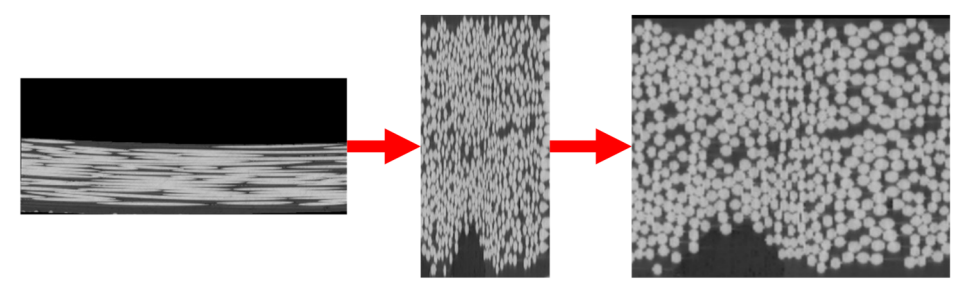


Figure 1. Process of rotating and scaling the 90-degree images.

#### **Automotive Scans**

The automotive-grade specimens were manufactured at the Institute for Textile Technology at RWTH University from Toho Tenax STS40 F13 48k tows. These specimens were made with the sole intent of bulk manufacturing. The tows were infiltrated with Hexion Epikote RIMR 135 with an Epikure RIMH curing agent. The tow was infiltrated using a VARTM process. The specimens were scanned at the European Synchrotron Radiation Facility. Scans were at a resolution of 0.332  $\mu m \,/\, vx$ , with 2048 px in the fiber direction and 2098 px in the transverse directions.

#### **Fiber Path Detection**

Each sample was analyzed using a MATLAB script in which the locations of each fiber in space were determined. Fibers were detected in each sectional image using "imfindcircles", a built-in function which uses a circular Hough Transform to find circles within a given image. Data objects were utilized to store information about each fiber due to their functionality and inherently organizable structure. The y-z coordinates of each found fiber in each cross-section, along with the radii, were stored as properties of "circle" objects. These were then stored as a stacks, effectively saving each cross-section as a stack of circles rather than a stack of images.

Fibers were "created" by combining the coordinates for each circle in each cross-section into one "fiber" object. Given the small spacing between images (0.3 um) the assumption was made that the fibers meander very little between sections. In other words, the fiber position in one cross-section is almost certainly the coordinate nearest the position in the previous section. With this assumption in mind, a nearest neighbor search algorithm was used to stitch the fibers together. Coordinates less than half of the mean fiber radius from the image border were removed to ensure all fibers analyzed were captured fully (i.e. to prevent incomplete fiber data). The data was further conditioned by removing the mean angular twist of all fibers from the global angular twist of the sample. The mean fiber radius was also used as the principal fiber radius for all further analyses.

The fiber coordinates were smoothed using a second order Savitzky-Golay filter, chosen for its tendency to preserve the overall shape of a curve. This ensured that the transition between circles was both smooth and continuous. After smoothing the fiber objects were adjoined into a single "bundle" object and multiplied by the corresponding image resolution to produce the actual coordinates in micrometers. Figure 2 shows the entire process of detecting and saving fibers.

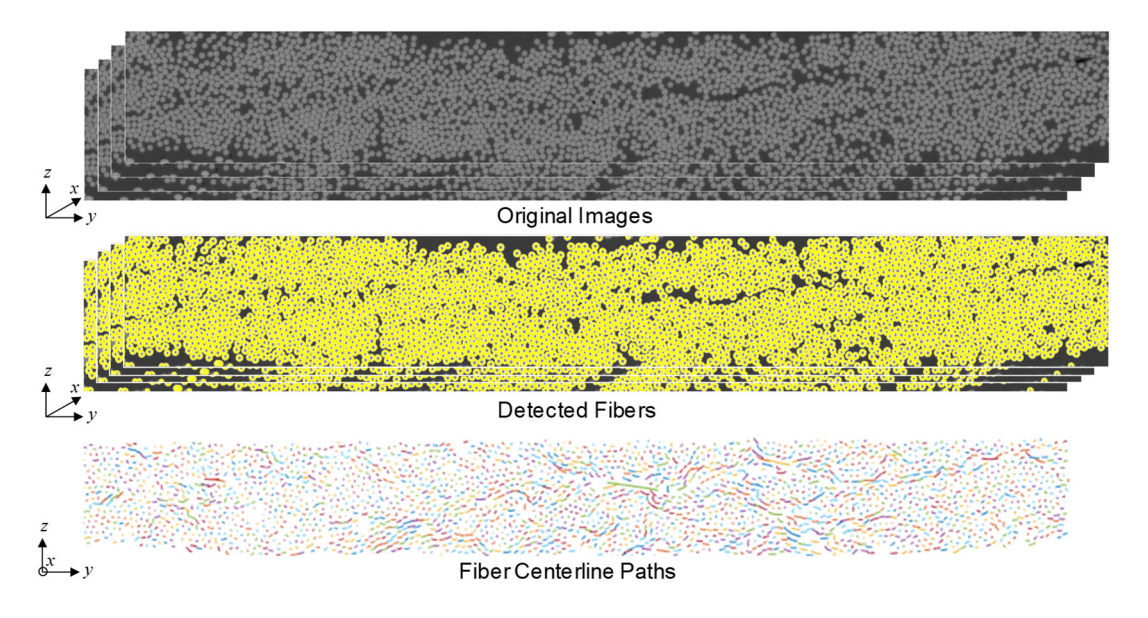


Figure 2. A collection of cross-sectional images of a composite were analyzed and the fiber centerline paths were determined.

# **Statistical Analysis**

The statistical metrics used were taken from Fast et al [4]. These were local fiber volume fraction, local fiber polar angle, and fiber metric correlation length. These metrics will be described below.

## LOCAL FIBER VOLUME FRACTION, $V_F$

The fiber volume fraction is a local metric defined as the ratio between a fiber's cross-sectional area and the area between itself and neighboring fibers. The area between a fiber and all neighboring fibers is referred to as a "cell". Cells are found using a Voronoi Tessellation (Figure 3a) in MATLAB for each cross-section. A Voronoi tessellation takes a set of points on a plane (e.g. the centers of all circles in a cross-section) and determines all cells where the points within the cell are closer to a single point in the set than any other. The cells found form a mosaic of the original plane.

To compare local fiber volume fraction distributions, histogram plots were constructed for each specimen. Figure 3b shows a typical specimen for the 0-degree layers of the Aerospace-grade composite.

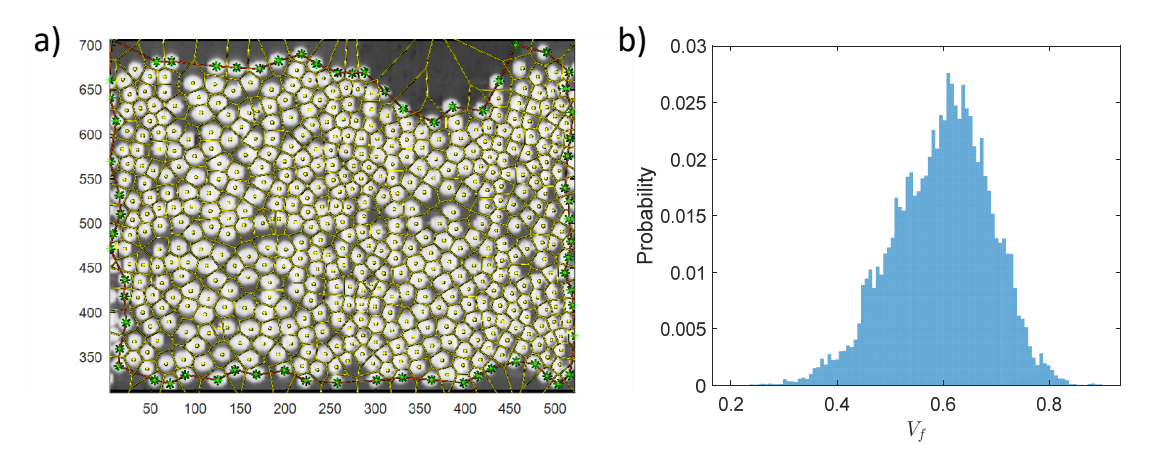


Figure 3. Typical volume fraction calculation using a) Voronoi tessellation to segment the sample and b) histogram plot of the local volume fractions of each cell.

### POLAR ANGLE

The polar angle  $\gamma$  is the angle between the x-axis (parallel with the fiber direction) and a point on the fiber. The polar angle is calculated using the following formula:

$$\gamma = \cos^{-1} \frac{X(i+1,1, j) - X(i,1,j)}{L}$$
 (1)

where X is the location of the fiber in space and L is the arc length between successive points along the same fiber. The second index of X is set to "1" to denote that the equation is "sweeping" through the x-direction.

To compare local fiber volume fraction distributions, histogram plots were constructed for each specimen and fit to a function. Figure 4 shows a typical specimen for the 0-degree layers of the Aerospace-grade composite.

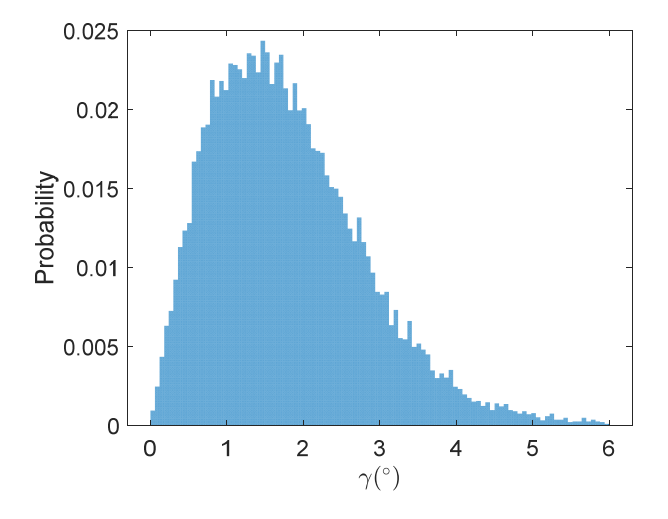


Figure 4. Typical aerospace-grade specimen for the polar angle.

## **CORRELATION LENGTH**

The correlation length C for a given parameter is defined here as the point at which the value of Pearson's Correlation Coefficient R drops below 0.5. Due to their relatively short lengths, the original aerospace-grade specimens do not permit the determination of correlation lengths. Figure 5 shows a typical specimen for the automotive grade composite.

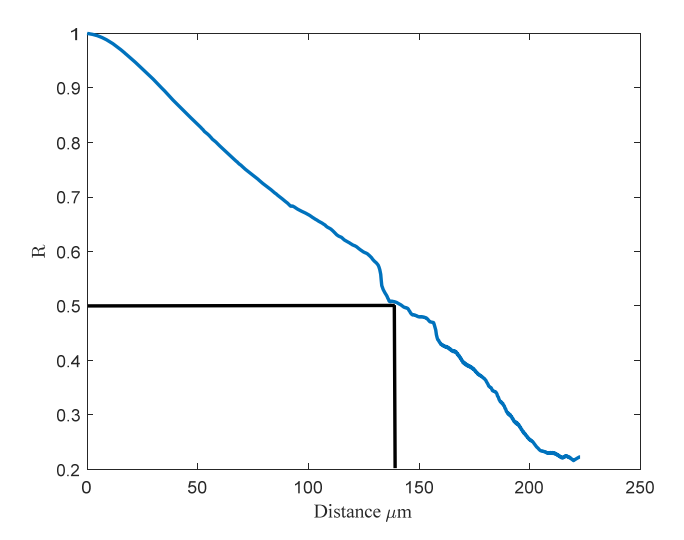


Figure 5. Correlation length determination for the local volume fraction of an automotive specimen.

#### RESULTS AND DISCUSSION

Scans of long Aerospace and Automotive-grade composites were compared with each other to highlight some aspects that differentiate the two. The three metrics defined here along with a qualitative comparison of the fiber centerline paths is presented here.

## FIBER VOLUME FRACTION

Figure 6 shows the histograms of the probability density of the local fiber volume fraction of both the long aerospace samples and the automotive sample. Consistent with past studies, the aerospace samples have a higher average local volume fraction than the automotive samples. It is worth noting, however, that the average local volume fraction for the 90-degree layers is still lower than that of the 0-degree layers measured in the past. This is likely due to the residual amount of distortion left over from the image conditioning process, causing certain regions to appear less dense than they actually are.

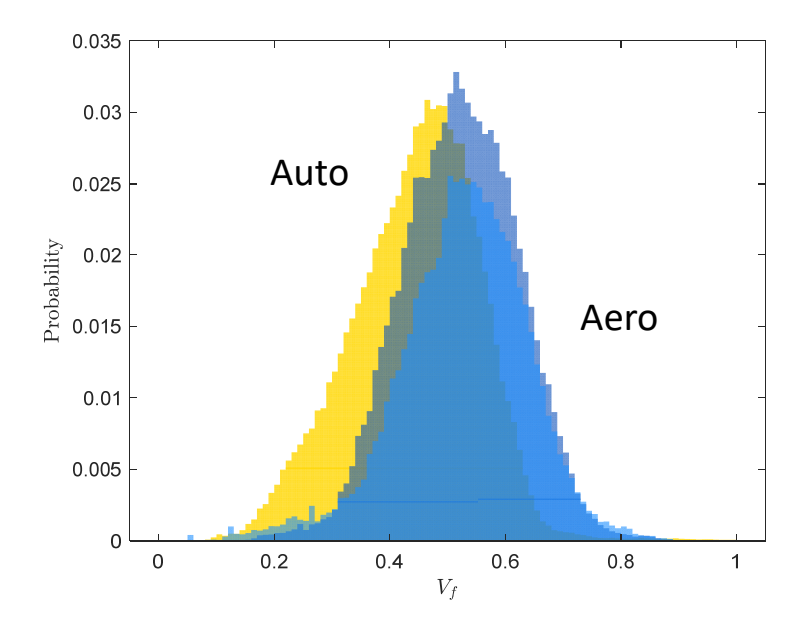


Figure 6. Comparison of the histograms of the fiber volume fraction for two 90-degree layers of an aerospace-grade composite and automotive-grade composite.

## FIBER POLAR ANGLE

Figure 7 shows the histograms of the probability density of the polar angle of both the long aerospace-grade samples and the automotive-grade samples. The first observation is that the range for the aero samples is much larger than that of the automotive sample. The wide range of the aero specimens is inconsistent with historical results from the 0-degree layers of the same material, which were much narrower than the automotive specimen. The main cause of this is likely the curved geometry of the specimen: the 0-degree layers all lay perpendicular to the curvature of the bracket, while the 90-degree layers move along its bend.

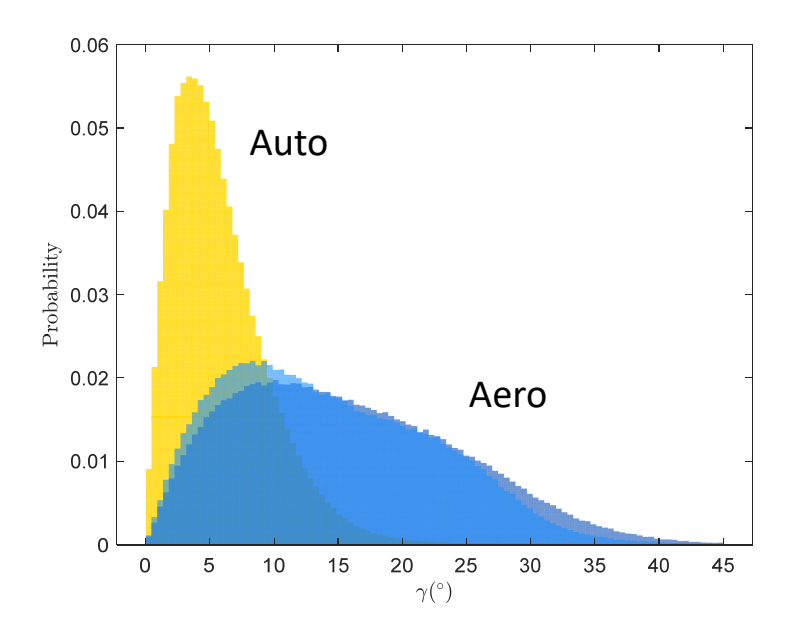


Figure 7. Comparison of the histograms of the polar angle for two 90-degree layers of an aerospace-grade composite and automotive-grade composite.

# **CORRELATION LENGTH**

The metric chosen for determination of a correlation length was the local fiber volume fraction due to its relative insensitivity to noise in the fiber position data. Figure 8 shows the comparison of R versus position along the fiber direction. The correlation lengths for the two aerospace samples were 176 um and 250 um, while the value for the automotive samples was 432 um. The main observation here, in the context of volume fraction, is that the aerospace-grade specimen requires a significantly less distance to characterize than the automotive-grade specimen. This observation is consistent with the trend observed in Fast et al [4]: the samples with the higher compaction produce smaller characteristic lengths than those with less compaction.

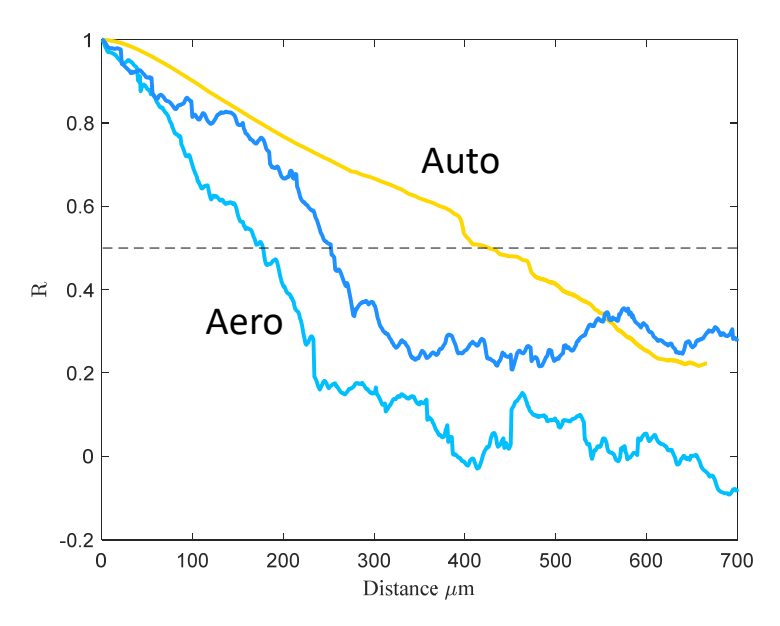


Figure 8. Comparison of Pearson's Correlation Coefficient for the two 90-degree layer aerospace samples and the automotive sample.

#### **CONCLUSIONS**

This study compared a few select metrics used to describe the fiber microstructure of composites taken from aerospace and automotive-grade materials. The purpose of this comparison is to work towards building a method for determining a 3-D length scale for modeling RVEs. The main challenge in this endeavor is obtaining CT samples that extend beyond the lengths typically found. The major takeaway from this study, however, is that the way in which parts are manufactured gives rise to certain correlation lengths for various metrics. Consequentially, these scales need to be considered in the modeling of microstructures. This can aid in not only tailoring manufacturing to get the lowest-cost part with the required properties, but also in ensuring statistical equivalence of artificially generated 3-D microstructures.

#### REFERENCES

- Sanei SHR, Fertig III RS (2015) Uncorrelated volume element for stochastic modeling of microstructures based on local fiber volume fraction variation. Composites Science and Technology 117:191–198. doi: 10.1016/j.compscitech.2015.06.010
- Sanei SHR, Barsotti EJ, Leonhardt D, Fertig RS (2017) Characterization, synthetic generation, and statistical equivalence of composite microstructures. Journal of Composite Materials 51:1817–1829. doi: 10.1177/0021998316662133
- 3. Czabaj MW, Riccio ML, Whitacre WW (2014) Numerical reconstruction of graphite/epoxy composite microstructure based on sub-micron resolution X-ray computed tomography. Composites Science and Technology 105:174–182. doi: 10.1016/j.compscitech.2014.10.017
- Fast T, Scott AE, Bale HA, Cox BN (2015) Topological and Euclidean metrics reveal spatially nonuniform structure in the entanglement of stochastic fiber bundles. J Mater Sci 50:2370–2398. doi: 10.1007/s10853-014-8766-2